

Hole spectral functions of LaMnO₃

Wei-Guo Yin^{1,2}, Hai-Qing Lin¹, and Chang-De Gong²

¹*Department of Physics, The Chinese University of Hong Kong, Sha Tin, Hong Kong, People's Republic of China*

²*National Key Laboratory of Solid States of Microstructure, Nanjing University, Nanjing 210093, People's Republic of China*
(November 24, 2000)

By use of the orbital t - J model, we calculate the photoemission spectra of LaMnO₃ using the exact diagonalization technique, and interpret our numerics quite well in the orbital-polaron scenario where the scattering between holes and orbital excitations is treated within the self-consistent Born approximation. The quasiparticle bandwidth is found to be of the order of J and t in the purely Coulombic and Jahn-Teller phononic model, respectively. We suggest that angle-resolved photoemission spectroscopy experiments allow one to distinguish between the orbital-polaron scenario and the Jahn-Teller polaron scenario.

PACS numbers: 75.30.Vn, 71.10.-w, 75.10.-b, 75.40.Mg

Orbital Physics is a key concept for recent intensive studies on transition-metal oxides [1], especially on manganese oxides with perovskite structure $R_{1-x}A_x\text{MnO}_3$ ($R = \text{La, Pr, Nd, Sm}$ and $A = \text{Ca, Sr, Ba}$) due to the discovery of colossal magnetoresistance in this class of materials. Mn^{3+} in RMnO_3 has four d electrons of which three are put into the t_{2g} orbitals and form an $S = 3/2$ localized spin, and the mobile one occupies one of the e_g orbitals ($d_{x^2-y^2}$ and $d_{3z^2-r^2}$). This e_g orbital degree of freedom may cause new phenomena through strong coupling with charge, spin, and lattice dynamics [2]. For example, alternating orbital order was observed in the ferromagnetic (FM) planes of A-type antiferromagnetic (AF) LaMnO₃ [3] and uniform $x^2 - y^2$ orbital order in A-type AF $\text{Pr}_{1/2}\text{Sr}_{1/2}\text{MnO}_3$ [4], while orbital liquid was proposed to exist in metallic FM $\text{La}_{1-x}\text{Sr}_x\text{MnO}_3$ ($x > 0.2$) [5]. These discoveries attract attention to the orbital correlation, dynamics and order-disorder transition. An essential first step is to understand the motion of a hole in an orbital ordered system such as the FM planes of LaMnO₃ [6]. We address it in this Letter.

Orbital ordering in LaMnO₃ can be induced by either the Jahn-Teller (JT) lattice distortion originating from the degeneracy of the e_g orbitals [7,8,9] or the intra-atomic Coulomb interaction in the e_g orbitals [9,10,11,12,13]. In the latter mechanism, the Coulomb interaction eliminates doubly occupied sites and results in the so-called *orbital* t - J model, a purely electronic Hamiltonian describing the orbital sector of physics of LaMnO₃. The model was initially derived by Kugel and Khomskii [10] and has been recently studied within mean field theory by Ishihara *et al.* [11] and via a finite-temperature diagonalization method by Horsch *et al.* [12]. The experimentally observed orbital ordering in LaMnO₃ [3] was reproduced by use of this model [12]. However, it can be also attributed to Jahn-Teller polarons [7,13]. In this Letter, we take the orbital t - J model as a starting point and discuss the JT effect later.

We first calculate photoemission spectra for the orbital t - J model using the exact diagonalization technique

(ED). The experimental counterpart of this problem is angle-resolved photoemission spectroscopy (ARPES) measurements. ARPES experiments have not yet been reported in this doping regime. Thus, we perform here computational experiments to explore unbiased information. Then, we satisfactorily interpret the outcome of such experiments in an *orbital-polaron* picture where the scattering between holes and orbital excitations is treated within the self-consistent Born approximation. Furthermore, we point out that although the JT lattice distortion leads to a large gap in the orbital excitation spectrum and thus resists the formation of the orbital-polaron, the hole can move almost freely through the orbital-flip process. The quasiparticle bandwidth is of the order of J (t) in the purely Coulombic (Jahn-Teller phononic) model, respectively. Our results indicate that ARPES may provide a possible approach to distinguish between the Coulombic scenario and the Jahn-Teller scenario.

The orbital t - J model is [10,11,12]

$$H = - \sum_{\langle \mathbf{ij} \rangle \| ab} (t_{ij}^{ab} \tilde{d}_{ia}^\dagger \tilde{d}_{jb} + \text{H.c.}) + \frac{J}{2} \sum_{\langle \mathbf{ij} \rangle \|} [T_i^z T_j^z + 3T_i^x T_j^x \mp \sqrt{3}(T_i^x T_j^z + T_i^z T_j^x)], \quad (1)$$

where $\tilde{d}_{ia}^\dagger = d_{ia}^\dagger(1 - n_{i\bar{a}})$ is the constrained fermion operator for the e_g electron at orbital a . $T_i^z = (\tilde{d}_{i\uparrow}^\dagger \tilde{d}_{i\uparrow} - \tilde{d}_{i\downarrow}^\dagger \tilde{d}_{i\downarrow})/2$ and $T_i^x = (\tilde{d}_{i\uparrow}^\dagger \tilde{d}_{i\downarrow} + \tilde{d}_{i\downarrow}^\dagger \tilde{d}_{i\uparrow})/2$ are orbital-pseudospin operators with $|\uparrow\rangle = d_{x^2-y^2}$ and $|\downarrow\rangle = d_{3z^2-r^2}$. The anisotropic transfer matrix elements are $t_{ij}^{\uparrow\uparrow} = 3t/4$, $t_{ij}^{\downarrow\downarrow} = t/4$, and $t_{ij}^{\uparrow\downarrow} = t_{ij}^{\downarrow\uparrow} = \mp\sqrt{3}t/4$, here the \mp sign distinguishes hopping along the x and y directions. The orbital superexchange interaction $J = t^2/(U - J')$ with U (J') being the interorbital Coulomb (exchange) integral [11,12]. In LaMnO₃, the realistic parameters are estimated from photoemission experiments [11,14] to be $t \sim 0.72$ eV, $U \sim 5$ eV, $J' \sim 2$ eV, thus $J \simeq 0.24t$.

The photoemission spectrum (PES) $\langle \tilde{d}_{ka}^\dagger \tilde{d}_{ka} \rangle_\omega$ [15] is calculated by using the standard Lanczos algorithm [16]. There are two bands and we find $\langle \tilde{d}_{k\downarrow}^\dagger \tilde{d}_{k\downarrow} \rangle_\omega =$

$\langle \tilde{d}_{\mathbf{k}+\mathbf{Q}}^\dagger \tilde{d}_{\mathbf{k}+\mathbf{Q}} \rangle_\omega$ with $\mathbf{Q} = (\pi, \pi)$. Fig. 1 shows the PES $\langle \tilde{d}_{\mathbf{k}\downarrow}^\dagger \tilde{d}_{\mathbf{k}\downarrow} \rangle_\omega$ of the ground state of the 16-site cluster at half filling. At any \mathbf{k} , there is a well-defined quasiparticle pole (i.e., zero orbital-wave) at the low energy side which is well separated from a broad, incoherent, multiple-orbital-wave background extending to the full free-electron bandwidth. The bottom and the top of the quasiparticle (QP) band locate at $(0,0)$ and (π, π) , respectively. The QP bandwidth of the order of J is much more narrow than the free-electron bandwidth. Note that all momenta belonging to the noninteracting 2D Fermi surface $\cos k_x + \cos k_y = 0$ are no longer degenerate despite their close proximity in energy. Correspondingly, the van Hove singularity in the density of states is weakened in the orbital t - J model.

Since the mixed terms $\propto T_i^x T_j^z + T_i^z T_j^x$ in the Hamiltonian (1) could contribute only in higher order orbital-wave theory than the linear one, it is interesting to perform similar calculations using the ED technique for the simplified Hamiltonian without these terms, which has been referred to as “the truncated Hamiltonian” by Brink *et al.* in their study of the purely orbital J model [12]. This could let us investigate the contribution of higher order orbital excitations to the QP behavior. Fig. 1 also illustrates the PES for the truncated Hamiltonian. The overall line shape of the PES remains almost unchanged but a slight shift to a higher energy. The prominent influence of higher order orbital excitations is that they suppress the heights of the quasiparticle peaks and thus weaken the QP spectral weights. We therefore conclude that as far as the QP dispersion relation is concerned, higher order orbital excitations can be neglected. The resultant QP dispersions are displayed in Fig. 2.

To get the physical insight of the above numerics, we perform an analytical calculation of the QP spectral functions in an *orbital-polaron* scenario. The J term induces the orbital Néel state, i.e., the alternation of orthogonal orbitals in the ground state. Here we analogize our problem to that of a hole moving in the AF spin background, an essential problem in the field of high-temperature superconductivity [17]. The latter can be accurately understood in the spin-polaron scenario where holes are described as spinless fermions (holons) and spins as hard-core bosons. The scattering between holes and spin-wave excitations is treated within the self-consistent Born approximation (SCBA) [17]. In the SCBA, higher order spin-wave excitations are also neglected, consistent with our ED results. Hence, we expect that our numerics may be interpreted in a similar way.

In LaMnO₃, alternatingly occupied orbitals on the two sublattices are oriented in the FM planes: $(|\uparrow\rangle + |\downarrow\rangle)/\sqrt{2}$ and $(|\uparrow\rangle - |\downarrow\rangle)/\sqrt{2}$ [3,12]. This state is different from the alternating directional orbitals $3x^2 - r^2$ and $3y^2 - r^2$, which have been naively expected [11]. To obtain the Néel configuration $|T_i^z T_{i+1}^z T_{i+2}^z T_{i+3}^z \dots\rangle = |\downarrow\uparrow\downarrow\uparrow \dots\rangle$ in

a new orbital basis, we perform a uniform rotation of orbitals by 90° about the T^y axis: $\tilde{d}_{i\uparrow} \rightarrow (\tilde{d}_{i\uparrow} - \tilde{d}_{i\downarrow})/\sqrt{2}$, $\tilde{d}_{i\downarrow} \rightarrow (\tilde{d}_{i\uparrow} + \tilde{d}_{i\downarrow})/\sqrt{2}$, and thus $T_i^z \rightarrow -T_i^x$, $T_i^x \rightarrow T_i^z$. Note that in the new orbital basis, the interorbital transfer matrix element is changed to $(t_{ij}^{\uparrow\uparrow} - t_{ij}^{\downarrow\downarrow})/2$. It is the imbalance between the $d_{x^2-y^2} - d_{x^2-y^2}$ hopping and the $d_{3z^2-r^2} - d_{3z^2-r^2}$ hopping that gives rise to the interorbital hopping in the rotated basis and causes the bare hole dispersion as shown below. Orbital excitations can be described within the linear spin-wave theory by defining $T_i^+ = \bar{a}_i^\dagger$, $T_i^z = \bar{a}_i^\dagger \bar{a}_i - \frac{1}{2}$ on the \downarrow sublattice, and $T_j^+ = \bar{b}_j$, $T_j^z = \frac{1}{2} - \bar{b}_j^\dagger \bar{b}_j$ on the \uparrow sublattice [12]. Here \bar{a}_i and \bar{b}_j are hard-core boson operators. Considering the orbital Néel state as the vacuum state, we define holon operators \tilde{h}_i (\tilde{f}_j) similar to those in the spin-polaron scenario [17] so that $\tilde{d}_{i\uparrow} = \tilde{h}_i^\dagger \bar{a}_i$, $\tilde{d}_{i\downarrow} = \tilde{h}_i^\dagger$ on the \downarrow sublattice and $\tilde{d}_{j\downarrow} = \tilde{f}_j^\dagger \bar{b}_j$, $\tilde{d}_{j\uparrow} = \tilde{f}_j^\dagger$ on the \uparrow sublattice.

Introducing new fermion operators $\{f_{\mathbf{k}}, h_{\mathbf{k}}\}$ in the momentum space $\tilde{f}_{\mathbf{k}} = (f_{\mathbf{k}} + h_{\mathbf{k}})/\sqrt{2}$, $\tilde{h}_{\mathbf{k}} = (f_{\mathbf{k}} - h_{\mathbf{k}})/\sqrt{2}$, we arrive at an effective orbital-polaron Hamiltonian

$$H_{\text{eff}} = \sum_{\mathbf{k}} \varepsilon_{\mathbf{k}} (f_{\mathbf{k}}^\dagger f_{\mathbf{k}} - h_{\mathbf{k}}^\dagger h_{\mathbf{k}}) + \sum_{\mathbf{q}} (\omega_{\mathbf{q}}^- \alpha_{\mathbf{q}}^\dagger \alpha_{\mathbf{q}} + \omega_{\mathbf{q}}^+ \beta_{\mathbf{q}}^\dagger \beta_{\mathbf{q}}) \\ + \sum_{\mathbf{kq}} (f_{\mathbf{k}}^\dagger f_{\mathbf{k}-\mathbf{q}} - h_{\mathbf{k}}^\dagger h_{\mathbf{k}-\mathbf{q}}) (g_{\mathbf{kq}}^\beta \beta_{\mathbf{q}} + g_{\mathbf{kq}}^\alpha \alpha_{\mathbf{q}}) + \text{H.c.} \quad (2) \\ + \sum_{\mathbf{kq}} (h_{\mathbf{k}}^\dagger f_{\mathbf{k}-\mathbf{q}} - f_{\mathbf{k}}^\dagger h_{\mathbf{k}-\mathbf{q}}) (\rho_{\mathbf{kq}}^\beta \beta_{\mathbf{q}} + \rho_{\mathbf{kq}}^\alpha \alpha_{\mathbf{q}}) + \text{H.c.},$$

where the bare hole dispersion is $\varepsilon_{\mathbf{k}} = -t\gamma_{\mathbf{k}}$. The holon-orbital-wave coupling functions are $g_{\mathbf{kq}}^\beta = \frac{2t}{\sqrt{N}}(\gamma_{\mathbf{k}} v_{\mathbf{q}}^+ + \gamma_{\mathbf{k}-\mathbf{q}} u_{\mathbf{q}}^+)$, $\rho_{\mathbf{kq}}^\beta = -\frac{\sqrt{3}t}{\sqrt{N}}(\eta_{\mathbf{k}} v_{\mathbf{q}}^+ - \eta_{\mathbf{k}-\mathbf{q}} u_{\mathbf{q}}^+)$, $\rho_{\mathbf{kq}}^\alpha = g_{\mathbf{k},\mathbf{q}+\mathbf{Q}}^\beta$ and $g_{\mathbf{kq}}^\alpha = \rho_{\mathbf{k},\mathbf{q}+\mathbf{Q}}^\beta$ with $\gamma_{\mathbf{k}} = (\cos k_x + \cos k_y)/2$, $\eta_{\mathbf{k}} = (\cos k_x - \cos k_y)/2$, and

$$u_{\mathbf{q}}^\pm = \{[(A_{\mathbf{q}} \pm B_{\mathbf{q}})/\omega_{\mathbf{q}}^\pm + 1]/2\}^{1/2}, \quad (3)$$

$$v_{\mathbf{q}}^\pm = -\text{sgn}(\pm B_{\mathbf{q}}) \{[(A_{\mathbf{q}} \pm B_{\mathbf{q}})/\omega_{\mathbf{q}}^\pm - 1]/2\}^{1/2}. \quad (4)$$

Here $A_{\mathbf{q}} = 3J$ and $B_{\mathbf{q}} = J\gamma_{\mathbf{q}}/2$. The $\alpha_{\mathbf{q}}$'s ($\beta_{\mathbf{q}}$'s) are orbital-wave operators, $\bar{a}_{\mathbf{q}} = \frac{1}{\sqrt{2}}(u_{\mathbf{q}}^+ \beta_{\mathbf{q}} + v_{\mathbf{q}}^+ \beta_{-\mathbf{q}}^\dagger + u_{\mathbf{q}}^- \alpha_{\mathbf{q}} + v_{\mathbf{q}}^- \alpha_{-\mathbf{q}}^\dagger)$, $\bar{b}_{\mathbf{q}} = \frac{1}{\sqrt{2}}(u_{\mathbf{q}}^+ \beta_{\mathbf{q}} + v_{\mathbf{q}}^+ \beta_{-\mathbf{q}}^\dagger - u_{\mathbf{q}}^- \alpha_{\mathbf{q}} - v_{\mathbf{q}}^- \alpha_{-\mathbf{q}}^\dagger)$, with dispersion $\omega_{\mathbf{q}}^\pm = \sqrt{A_{\mathbf{q}}(A_{\mathbf{q}} \pm 2B_{\mathbf{q}})}$.

The holon Green's functions $G_{f,h}(\mathbf{k}, \omega) = [\omega \mp \varepsilon_{\mathbf{k}} - \Sigma_{f,h}(\mathbf{k}, \omega)]^{-1}$ are calculated within the SCBA [17]. Note that $\Sigma_f(\mathbf{k} + \mathbf{Q}, \omega) = \Sigma_h(\mathbf{k}, \omega)$ and $G_f(\mathbf{k} + \mathbf{Q}, \omega) = G_h(\mathbf{k}, \omega)$ with $\mathbf{Q} = (\pi, \pi)$. The self-energy is thus of form

$$\Sigma_f(\mathbf{k}, \omega) = \sum_{\mathbf{q}} [(g_{\mathbf{kq}}^\beta)^2 G_f(\mathbf{k} - \mathbf{q}, \omega - \omega_{\mathbf{q}}^+) \\ + (\rho_{\mathbf{kq}}^\beta)^2 G_f(\mathbf{k} + \mathbf{Q} - \mathbf{q}, \omega - \omega_{\mathbf{q}}^+)], \quad (5)$$

where \sum' means to sum over the first Brillouin zone.

The QP spectral functions $A_f(\mathbf{k}, \omega) = -\frac{1}{\pi} \text{Im } G_f(\mathbf{k}, \omega)$ are shown in Fig. 3 [18]. The QP dispersion $E_{\mathbf{k}}^f =$

$\varepsilon_{\mathbf{k}} + \Sigma_f(\mathbf{k}, E_{\mathbf{k}}^f)$ (see Fig. 2) and the spectral weights $Z(\mathbf{k}) = \left[1 - \frac{\partial \Sigma_f(\mathbf{k}, \omega)}{\partial \omega}\right]_{\omega=E_{\mathbf{k}}}^{-1}$ (see Table I). All of the SCBA results are in good agreement with the ED results, especially with those for the truncated Hamiltonian as expected. Therefore, the orbital-polaron scenario may provide a valuable scheme for further works on the orbital dynamics.

In the rest of this Letter, we discuss the Jahn-Teller effect on the quasiparticle band. Recently, Bała and Oleś suggested that a large gap in the orbital excitation spectrum induced by the JT lattice distortion might lead to a strong confinement of holes in lightly doped LaMnO₃ insulators [13]. This implies that the hole quasiparticle bandwidth is more narrow in the presence of JT phonons. We include the JT effect in the same way as Bała and Oleś [7,13] but we get a different result. The Jahn-Teller interaction considered here is [13]

$$H_{\text{JT}} = -2E_{\text{JT}}(\phi, \delta_x, \delta_z, u) \left(\sum_{\mathbf{i} \in A} T_{\mathbf{i}}^z - \sum_{\mathbf{j} \in B} T_{\mathbf{j}}^z \right). \quad (6)$$

Here $T_{\mathbf{i}}^z$ refers to the rotated basis. $E_{\text{JT}}(\phi, \delta_x, \delta_z, u) = \lambda[(\delta_x - \delta_z) \sin 2\phi - 2\sqrt{3}u \cos 2\phi]$ acts as a fictitious “magnetic field” in which ϕ is the tilting angle of pseudospins, and δ_x, δ_z, u characterize lattice distortions (in units of the lattice constant): $\delta_x(\delta_z)$ — uniform deformation along the x and y (z) directions, and u — oxygen ionic displacement along Mn-O-Mn bond in the xy plane [19]. The distorted lattice energy per Mn ion is $E_l(\delta_x, \delta_z, u) = K_1(\frac{1}{2}\delta_x^2 + 2u^2 + \frac{1}{4}\delta_z^2) + K_2(\delta_x^2 + \frac{1}{2}\delta_z^2)$ where $K_1(K_2)$ is the nearest-neighbor Mn-O (Mn-Mn) spring constant. To estimate the JT effect on the quasiparticle behavior, we may consider the case of $\phi = 0$ (i.e., no static distortions due to a tetragonal field) without loss of generality. In the classical ground state at $\phi = 0$, $E_{\text{JT}} = -3\lambda^2/K_1$. For the realistic parameters of LaMnO₃: the spring constant $K_1 = 200$ eV and the JT interaction parameter $\lambda \simeq 6$ eV [7,13], $E_{\text{JT}} = -0.54$ eV.

In order to calculate $E_{\mathbf{k}}^f$ in the presence of JT lattice distortion, all we have to modify the above derivation is to make the following replacement in (3) and (4): $A_{\mathbf{q}} \rightarrow 3J - 2E_{\text{JT}} = 3J + 6\lambda^2/K_1$. The JT interaction adds an Ising-like component to the excitations and induces a large gap in the orbital excitation spectrum. Thus, the JT effect stabilizes the orbital ordering.

The SCBA results on the 20×20 lattice are summarized in Table 1. The large gap in the orbital excitation spectrum induced by the JT lattice distortion does not weaken the QP bandwidth. Instead, at $\lambda = 6$ eV the QP bandwidth reaches 75 percent of the width ($2t$) of the bare hole dispersion $\varepsilon_{\mathbf{k}}$. Although the large gap in the orbital excitation spectrum resists the formation of the orbital polaron, the hole can move almost *freely* via the orbital-flip process in the rotated orbital basis. For $A_{\mathbf{q}} \gg t$ because of large J or large λ , Eq. (5) can be

solved analytically in perturbation theory. Most of the spectral weight, $1 - O(t^2/A_{\mathbf{q}}^2)$, appears in the quasiparticle part of $G_f(\mathbf{k}, \omega)$ which behaves indeed a bare dispersion $E_{\mathbf{k}}^f \simeq \varepsilon_{\mathbf{k}} - \sum_{\mathbf{q}} [(g_{\mathbf{kq}}^\beta)^2 + (\rho_{\mathbf{kq}}^\beta)^2] / \omega_{\mathbf{q}}^+ \simeq \varepsilon_{\mathbf{k}} - O(t^2/A_{\mathbf{q}})$. Fig. 4 shows the QP bandwidth W as a function of J . Without the JT interaction ($\lambda = 0$ eV), $W \simeq 2.2J$ scales with J in the range of $0.01 \leq J \leq 0.4$, and approaches to the width of the bare hole dispersion ($2t$) for large J . On the other hand, with strong JT interaction ($\lambda = 6$ eV), W is of the order of t in the whole range of J . These results reminisce those for one hole moving in the *spin* t - t' - J model (the t - t' - J_z model with large J_z), respectively, where the transfer to next nearest neighbors (t') provides the bare hole dispersion [15,16]. Therefore, the QP bandwidth for realistic J is of the order of t (J) in the presence (absence) of strong Jahn-Teller interaction. Our results can be tested by future ARPES experiments.

The authors thank P. W. Leung, F. C. Zhang, and H. Zheng for useful discussions. The ED program was implemented on the basis of C codes provided by P. W. Leung. W.G.Y. is supported by CUHK 4288/00P 2160148.

-
- [1] Y. Tokura and N. Nagaosa, Science **288**, 462 (2000); Y. Q. Li, M. Ma, D. N. Shi, and F. C. Zhang, Phys. Rev. Lett. **81**, 3527 (1998).
 - [2] R. Maezono, S. Ishihara, N. Nagaosa, Phys. Rev. B **58**, 11 583 (1998).
 - [3] Y. Murakami, J. P. Hill, D. Gibbs, M. Blume, I. Koyama, M. Tanaka, H. Kawata, T. Arima, Y. Tokura, and Y. Endoh, Phys. Rev. Lett. **81**, 582 (1998).
 - [4] H. Kawano, R. Kajimoto, H. Yoshizawa, Y. Tomioka, H. Kuwahara, and Y. Tokura, Phys. Rev. Lett. **78**, 4253 (1997).
 - [5] K. H. Kim, J. H. Jung, and T. W. Noh, Phys. Rev. Lett. **81**, 1517 (1998); M. Quijada, J. Černe, J. R. Simpson, H. D. Drew, K. H. Ahn, A. J. Millis, R. Shreekala, R. Ramesh, M. Rajeswari, and T. Venkatesan, Phys. Rev. B **58**, 16 093 (1998).
 - [6] Because of Hund’s rule, the spin of the mobile e_g electron is enforced to be parallel to the localized t_{2g} electrons, and the transfer integrals are normalized via the double-exchange mechanism [C. Zener, Phys. Rev. **82**, 403 (1951); P. W. Anderson and H. Hasegawa, Phys. Rev. **100**, 675 (1955)] by a factor of $\cos(\theta_{xy}/2)$ or $\cos(\theta_z/2)$ where θ_{xy}, θ_z are the angle between neighboring t_{2g} spins in the xy plane and in the z -direction, respectively. Thus, hole motion in the perfect A -type AF state ($\theta_{xy} = 0$ and $\theta_z = \pi$) can be considered as hole motion in the FM planes.
 - [7] A. J. Millis, Phys. Rev. B **53**, 8434 (1996); K. H. Ahn and A. J. Millis, *ibid.* **58**, 3697 (1998); J. Kanamori, J. Appl. Phys. **31**, 145 (1961).
 - [8] T. Hotta, S. Yunoki, M. Mayr, and E. Dagotto, Phys. Rev. B **60**, R15 009 (1999); A. Moreo, S. Yunoki, and E.

- Dagotto, Science **283**, 2034 (1999); S. Yunoki, A. Moreo, and E. Dagotto, Phys. Rev. Lett. **81**, 5612 (1998).
- [9] T. Hotta, A. L. Malvezzi, and E. Dagotto, Phys. Rev. B **62**, 9432 (2000).
- [10] K. I. Kugel and D. I. Khomskii, Zh. Éksp. Teor. Fiz. **64**, 1429 (1973) [Sov. Phys. JETP **37**, 725 (1973)].
- [11] S. Ishihara, J. Inoue, and S. Maekawa, Phys. Rev. B **55**, 8280 (1997); S. Ishihara, M. Yamanaka, and N. Nagaosa, *ibid.* **56**, 686 (1997); R. Kilian and G. Khaliullin, *ibid.* **58**, R11 841 (1998).
- [12] P. Horsch, J. Jaklic, and F. Mack, Phys. Rev. B **59**, 6217 (1999); J. van den Brink, P. Horsch, and F. Mack, *ibid.* **59**, 6795 (1999); F. Mack and P. Horsch, Phys. Rev. Lett. **82**, 3160 (1999).
- [13] J. Bała and A. M. Oleś, Phys. Rev. B **62**, R6085 (2000).
- [14] T. Saitoh, A. E. Bocquet, T. Mizokawa, H. Namatame, A. Fujimori, M. Abbate, Y. Takeda, and M. Takano, Phys. Rev. B **51**, 13 942 (1995).
- [15] Wei-Guo Yin, C. D. Gong, and P. W. Leung, Phys. Rev. Lett. **81**, 2534 (1998); P. W. Leung and R. J. Gooding, Phys. Rev. B **52**, R15 711 (1995).
- [16] E. Dagotto, Rev. Mod. Phys. **66**, 763 (1994).
- [17] S. Schmitt-Rink, C. M. Varma, and A. E. Ruckenstein, Phys. Rev. Lett. **60**, 2793 (1988); C. L. Kane, P. A. Lee, and N. Read, Phys. Rev. B **39**, 6880 (1989); G. Martinez and P. Horsch, *ibid.* **44**, 317 (1991); Z. Liu and E. Manousakis, *ibid.* **44**, 2414 (1991); Wei-Guo Yin, Biao Hao, and C. D. Gong, Phys. Lett. A **220**, 281 (1996).
- [18] In comparison with the ED results, we perform the following transformation for the SCBA results: $\omega \rightarrow \omega + \Delta E_J$ where $\Delta E_J = 0.43903t$ is the energy loss of the orbital background at one hole doping.
- [19] When a hole is present on site i , it attracts the surrounding oxygen ions equally, giving rise to a breathing distortion energy. Since the breathing mode does not distinguish between the e_g orbitals, it can be safely neglected in the present study.

TABLE I. Bandwidth W and spectral weights $Z(k)$ as a function of the Jahn-Teller interaction parameter λ . $J = 0.3t$.

λ (eV)	W/t	$Z(0,0)$	$Z(\pi/2, \pi/2)$	$Z(\pi, \pi)$	$Z(\pi, 0)$
0	0.65210	0.65989	0.37446	0.09774	0.39068
4	1.12691	0.79211	0.60401	0.30239	0.60701
6	1.49980	0.87222	0.77294	0.57996	0.77022
8	1.74565	0.92421	0.88066	0.80063	0.87943

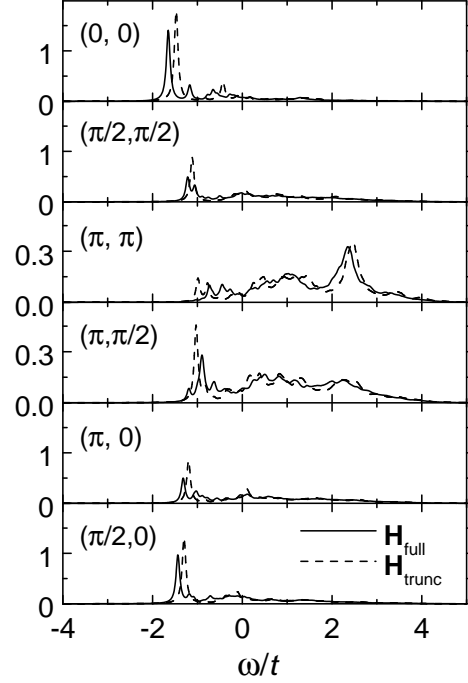


FIG. 1. The PES $\langle \tilde{d}_{\mathbf{k}\downarrow}^\dagger \tilde{d}_{\mathbf{k}\downarrow} \rangle_\omega$ for the orbital t - J model on the 4×4 cluster using the ED technique for the full Hamiltonian (solid lines) and the truncated Hamiltonian (dashed lines). Here $J = 0.3t$.

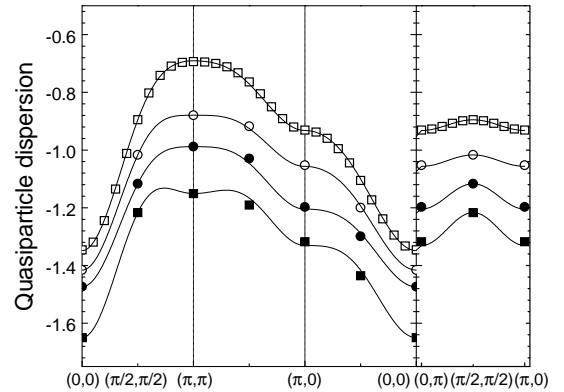


FIG. 2. Hole quasiparticle dispersion for the orbital t - J model with $J = 0.3t$: The ED results for the full Hamiltonian (solid squares) and the truncated Hamiltonian (solid circles); The SCBA results on the 4×4 cluster (open circles) and the 20×20 one (open squares). Solid lines are the fits using $E_{\mathbf{k}}^f = a_0 + a_1\gamma_{\mathbf{k}} + a_2 \cos k_x \cos k_y + a_3\gamma_{2\mathbf{k}}$.

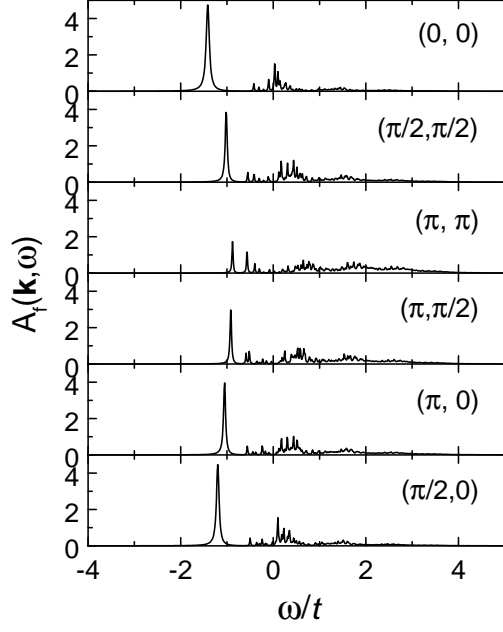


FIG. 3. The PES $A_f(\mathbf{k}, \omega)$ for the orbital t - J model on the 4×4 cluster calculated within the SCBA. Here $J = 0.3t$.

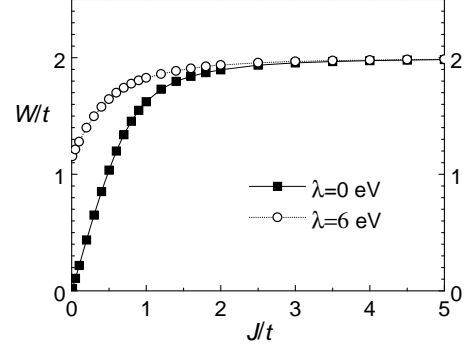


FIG. 4. The quasiparticle bandwidth W as a function of J at different Jahn-Teller interaction parameters: $\lambda = 0$ (solid squares) and $\lambda = 6$ eV (open circles). Calculations are performed on the 16×16 cluster within the SCBA.